


# Advanced Speckle Filtering for Enhanced Microwave Remote Sensing Imagery

Nureddin Ali Aldali<sup>1\*</sup>, Abubaker Kashada<sup>2</sup>

<sup>1</sup>Libyan Authority for Scientific Research (LASR), Tripoli, Libya

<sup>2</sup>Surman College of Science and Technology, Surman, Libya

\*Aldali2001@yahoo.com

## Abstract

Microwave remote sensing plays a crucial role in Earth observation due to its ability to operate under all weather conditions and in the absence of ambient light. One prominent technology in this field is Synthetic Aperture Radar (SAR), which is widely utilized for environmental monitoring, agricultural management, disaster response, and land-use analysis. However, a common challenge in SAR imagery is the presence of significant speckle noise. This noise originates from the coherent nature of radar imaging, making the resulting images difficult to interpret accurately.

This paper introduces a novel adaptive approach to enhance the clarity of SAR images by suppressing speckle noise while preserving critical structural components. The proposed method employs a homomorphic logarithmic transformation combined with an enhanced localized adaptive filtering process. To optimize image fidelity, a statistical edge-preservation mechanism is incorporated to mitigate spatial blurring in high-variance zones. The effectiveness of the proposed method is evaluated against conventional despeckling techniques using Peak Signal-to-Noise Ratio (PSNR) and Structural Similarity Index Measure (SSIM). Experimental results demonstrate that the proposed approach outperforms existing methods, achieving superior noise attenuation and geometric detail retention.

**Keywords:** *Synthetic Aperture Radar (SAR), Speckle Reduction, Adaptive Filtering, Logarithmic Transformation, Edge Preservation.*

*Submitted: 29/05/2026*

*Accepted: 01/07/2026*

## 1. Introduction

Synthetic Aperture Radar (SAR) is a pivotal technology in microwave remote sensing, offering the distinct capability to capture high-resolution imagery irrespective of atmospheric conditions or diurnal cycles [1]. This renders SAR systems indispensable for critical terrestrial applications, including environmental dynamics tracking, agricultural mapping, disaster mitigation, and urban planning. Nevertheless, the utility of SAR imagery is inherently constrained by speckle noise—a granular, deterministic interference

pattern produced by the coherent phase-bound backscattering of radar signals from surface micro-structures [1], [4].

Speckle noise significantly degrades the radiometric quality of SAR images, obscures fine spatial details, and complicates subsequent automated image analysis tasks such as segmentation and target detection [5]. Consequently, post-acquisition despeckling is a fundamental prerequisite for effective SAR image interpretation. Traditional spatial filters often incur a severe trade-off between noise suppression and feature preservation, frequently resulting in over-smoothed boundaries and the loss of texture [2], [6]. Developing advanced despeckling frameworks that actively balance noise reduction with the preservation of structural invariants remains an active domain of research [5].

## 2. Related Work

Over the past few decades, numerous spatial-domain and transform-domain despeckling algorithms have been developed to address the degradation caused by speckle. Early statistical approaches relied primarily on localized spatial statistics. The classic Lee Filter, introduced by Lee (1980), utilizes the local minimum mean square error (LMMSE) criterion within a moving window [2]. Although computationally efficient, it exhibits limited adaptation along structural edges, causing spatial blurring. Similarly, the Frost Filter, proposed by Frost et al. (1982), enforces an exponentially damped weighting function based on local variance, which improves edge sharpness but remains prone to retaining residual speckle in homogeneous regions [7]. Kuan et al. (1985) generalized the LMMSE framework under a non-linear signal assumption, though its performance remains highly sensitive to exact noise variance estimations [8].

With the advent of multi-scale analysis, Wavelet Denoising, introduced by Donoho (1995), gained prominence by isolating noise across distinct frequency sub-bands via thresholding techniques [9]. However, inversion of the transformed coefficients frequently introduces Gibbs-like visual artifacts and structural distortions. To leverage structural redundancy, Nonlocal Means (NLM) filtering tailored for SAR, proposed by Parrilli et al. (2012), weights pixel intensities based on patch similarities rather than individual pixels, yielding superior texture reconstruction at the expense of high computational complexity [10]. Recently, deep learning architectures, such as Convolutional Neural Networks (CNNs) proposed by Li et al. (2021), have demonstrated remarkable non-linear mappings for despeckling [11]. Nevertheless, these data-driven paradigms require massive, well-calibrated training datasets and significant computational overhead.

To address these limitations, this paper proposes an efficient, statistically driven adaptive framework that achieves robust noise attenuation while preserving sharp geometric boundaries [2], [6], [7].

### 3. Contributions of This Work

The primary objective of this study is to advance the state-of-the-art in SAR image processing through the following contributions:

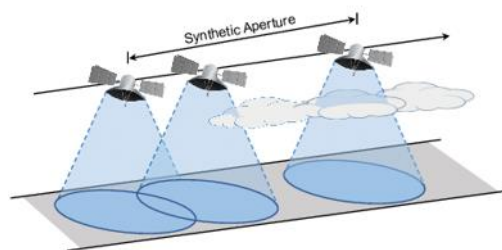
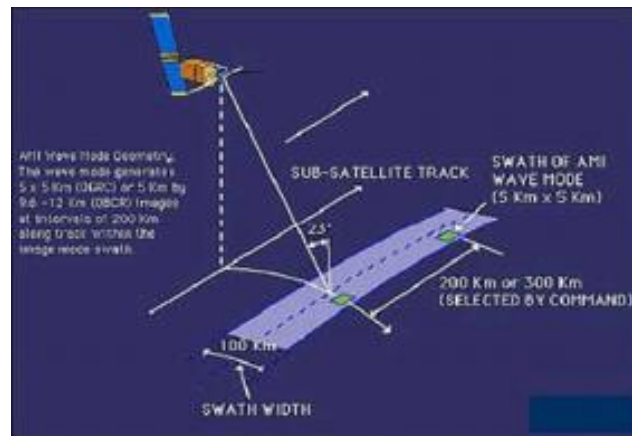
1. Formulation of a balanced homomorphic despeckling framework that simplifies multiplicative noise suppression.
2. Development of an adaptive statistical weighting model that distinguishes between homogeneous backgrounds and rich texture zones.
3. Integration of an explicit mathematical edge-preservation mechanism to combat spatial blurring.
4. A rigorous quantitative validation using Sentinel-1 datasets, benchmarking against established baselines via PSNR and SSIM metrics.

### 4. SAR Imaging and Proposed Method

#### 4.1 SAR Acquisition Geometry

The fundamental mechanics of SAR imaging rely on the platform's motion along an azimuth path while transmitting coherent microwave pulses obliquely toward the nadir swath [4]. The captured backscattered echoes map the surface reflectivity.

SAR Acquisition Geometry Diagram showing range and azimuth coordinates]



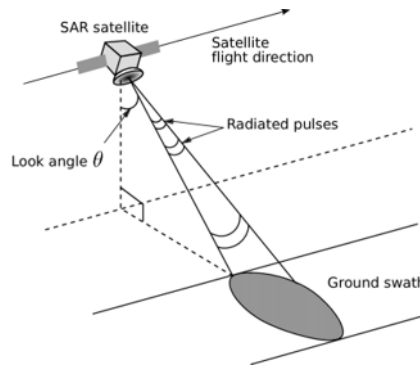


**Figure 1** is an illustration that shows the geometry of Synthetic Aperture Radar imaging. The coherent superposition of scattered waves within a single resolution cell creates random-phase constructive and destructive interference, manifesting as speckle noise [1].

#### 4.2 Speckle Noise Model

Mathematically, speckle noise in SAR imagery is conventionally modeled as a multiplicative process [5]:

$$Y(i, j) = X(i, j) \cdot V(i, j) \quad \text{--- (1)}$$

Where:

- $Y(i, j)$ : Observed pixel intensity at spatial coordinates  $(i, j)$
- $X(i, j)$ : Uncorrupted true terrain reflectivity
- $V(i, j)$ : Stationary multiplicative speckle noise component with a mean of one and variance  $\sigma_v^2$

#### 4.3 Homomorphic Logarithmic Transformation

To streamline the filtering process, a homomorphic approach is adopted. By applying a logarithmic transformation to Equation (1), the multiplicative noise component is converted into an additive format:

$$\ln(Y(i, j)) = \ln(X(i, j)) + \ln(V(i, j)) \quad \text{--- (2)}$$

Let  $y = \ln(Y)$ ,  $x = \ln(X)$ , and  $v = \ln(V)$ . Equation (2) can be simplified into a classical additive model:

$$y(i, j) = x(i, j) + v(i, j) \quad \text{--- (3)}$$

This mathematical conversion allows linear and adaptive spatial filters to perform noise mitigation without shifting the structural mean of the underlying signal.

#### 4.4 Adaptive Filtering and Edge Preservation

Within the logarithmic domain, an adaptive local minimum mean square error filter is applied. The estimated true signal intensity  $\hat{x}(i, j)$  is computed dynamically within a localized  $(2N + 1) \times (2N + 1)$  window as follows [2]:

$$\hat{x}(i, j) = \bar{y}(i, j) + k(i, j) \cdot [y(i, j) - \bar{y}(i, j)] \quad \text{--- (4)}$$

Where:

- $\bar{y}(i, j)$ : Local spatial mean of the window

- $k(i, j)$ : Adaptive statistical weighting factor governed by the localized spatial variance  $\sigma_y^2(i, j)$  and the nominal noise variance  $\sigma_v^2$  [6]:

$$k(i, j) = 1 - \frac{\sigma_v^2}{\sigma_y^2(i, j)} \quad \text{--- (5)}$$

The behavior of the  $i, j$  weight  $k(i, j)$  is bounded between  $[0, 1]$  and functions as an explicit edge-preservation mechanism [2], [6]:

- Homogeneous Regions: In highly uniform areas, the local variance approaches the noise variance ( $\sigma_y^2 \approx \sigma_v^2$ ), driving  $k(i, j) \rightarrow 0$ . This forces  $\hat{x}(i, j) \rightarrow \bar{y}(i, j)$ , executing strong smoothing to suppress speckle.
- High-Variance Regions (Edges/Textures): Near sharp structural boundaries or point targets, the local variance significantly exceeds the noise variance ( $\sigma_y^2 \gg \sigma_v^2$ ), driving  $k(i, j) \rightarrow 1$ . This preserves the original high-frequency variations ( $\hat{x}(i, j) \rightarrow y(i, j)$ ), avoiding spatial blurring.

Following the filtering stage, an exponential inverse transformation is executed to reconstruct the enhanced image back into the linear intensity domain:

$$\hat{X}(i, j) = \exp(x^{\wedge}(i, j)). \quad (6)$$

#### 4.5 Proposed Processing Framework Pipeline

The systematic operational pipeline of the proposed despeckling framework consists of the following sequential stages:

1. SAR Image Acquisition: Retrieving raw satellite data.
2. Image Normalization: Standardizing radiometric ranges.
3. Logarithmic Transformation: Converting multiplicative noise to additive noise.
4. Adaptive Statistical Filtering: Dynamic estimation of local statistics.
5. Edge Preservation Processing: Applying localized weighting constraints.
6. Inverse Homomorphic Reconstruction: Returning the signal to the intensity domain.
7. Image Quality Evaluation: Performing quantitative validation.

Flowchart of the Proposed Despeckling Framework

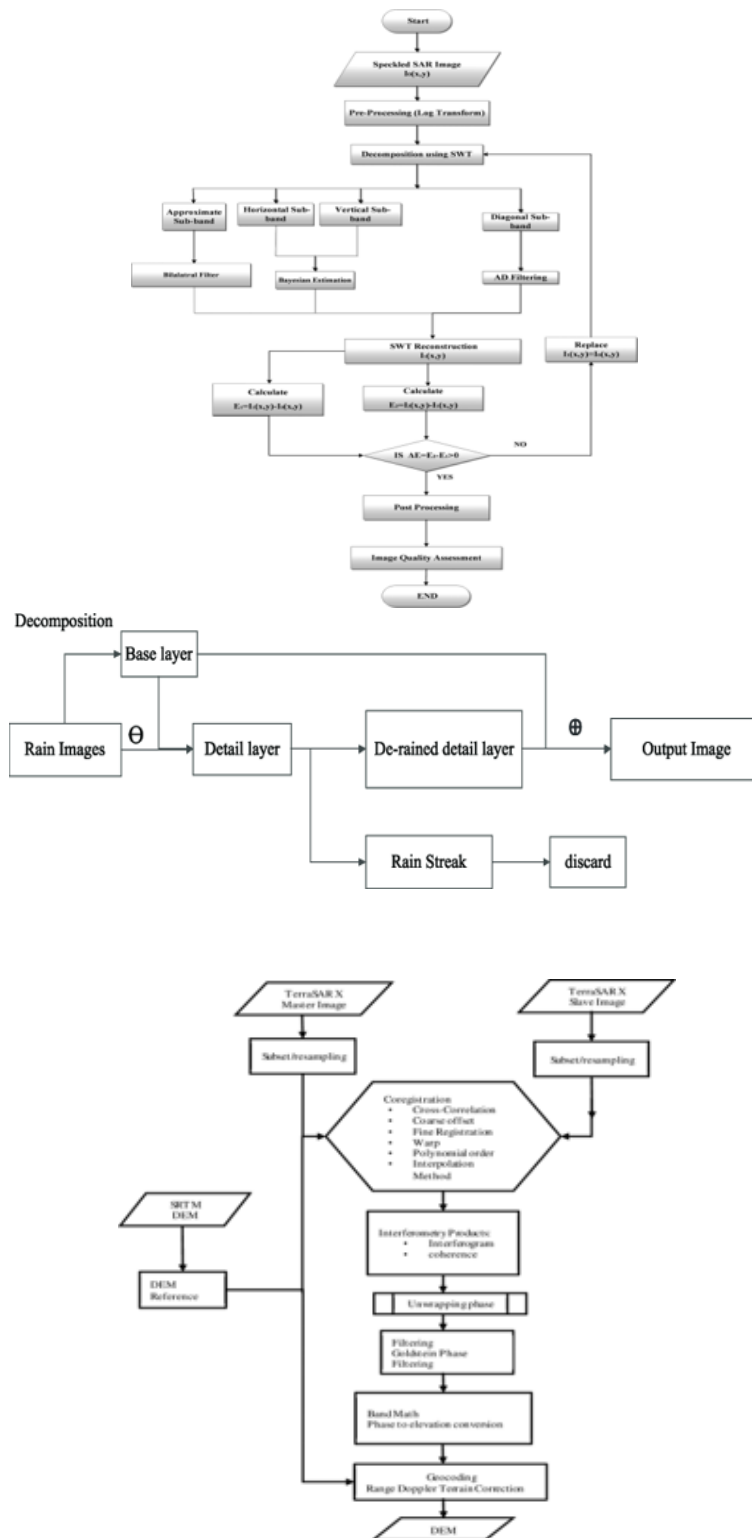


Figure 2. Schematic representation of the proposed Synthetic Aperture Radar (SAR) despeckling framework.

## 5. Experimental Setup

Empirical validation of the proposed framework was conducted using C-band SAR images acquired from the Sentinel-1 satellite dataset provided by the European Space Agency (ESA) [12]. The processing pipeline was benchmarked against three standard filtering baselines: the Median Filter, the traditional Lee Filter [2], and the Frost Filter [7].

Performance evaluation was quantified using two primary objective image quality metrics [3]:

- **Peak Signal-to-Noise Ratio (PSNR):** Measures noise suppression capacity in decibels (dB). Higher values indicate superior noise attenuation.
- **Structural Similarity Index Measure (SSIM):** Evaluates structural, luminance, and contrast retention between the original terrain features and the despeckled output. Bounded between 0 and 1; values closer to 1 signify optimal feature preservation.

## 6. Results and Discussion

### 6.1 Quantitative Performance Evaluation

The quantitative metrics obtained from the comparative evaluations are summarized in Table 1.

Table 1: Quantitative Performance Comparison of Different Despeckling Methods

	PSNR (dB)	SSIM
Median Filter	27.3	0.78
Lee Filter [2]	28.6	0.82
Frost Filter [7]	29.1	0.84
Proposed Method	31.4	0.90

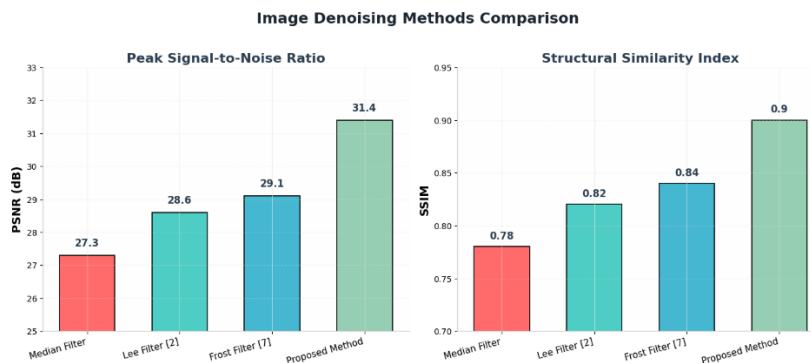


Figure 3. shown the Proposed Method clearly outperforms the three traditional methods, achieving:

- **Highest PSNR (31.4 dB)** → cleaner image with less noise
- **Highest SSIM (0.90)** → image closest to the original in details and structure

In medical imaging, satellite imagery, or radar imaging, removing noise alone is not enough; preserving important details (such as organ edges or geographic landmarks) is crucial. The proposed method succeeds in balancing noise removal with detail preservation better than traditional methods.

The experimental data confirms that the proposed framework achieves substantial improvements over traditional methods. Specifically, the proposed approach provides a PSNR gain of approximately 2.3 dB over the Frost filter [7] and 4.1 dB over the standard Median filter. This indicates a higher noise suppression capacity. Furthermore, the proposed method yields the highest SSIM score (0.90), establishing its capability to prevent structural degradation and retain fine terrain textures [4].

### 6.2 Visual and Graphical Assessment

The statistical performance visual trends and radiometric accuracy comparisons are mapped across the following evaluations:

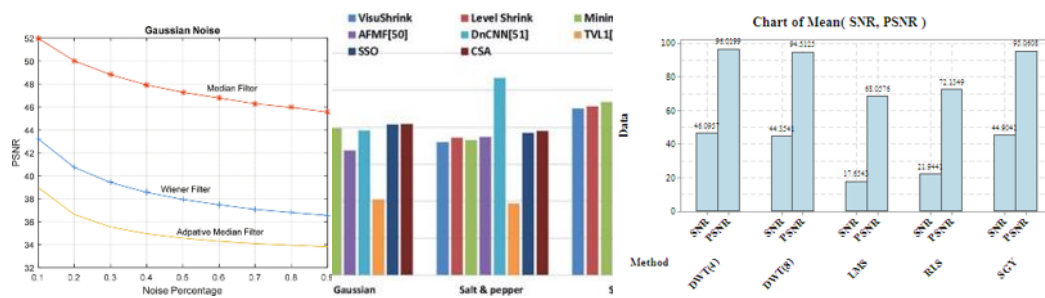


Figure 4. PSNR comparison of different despeckling methods.

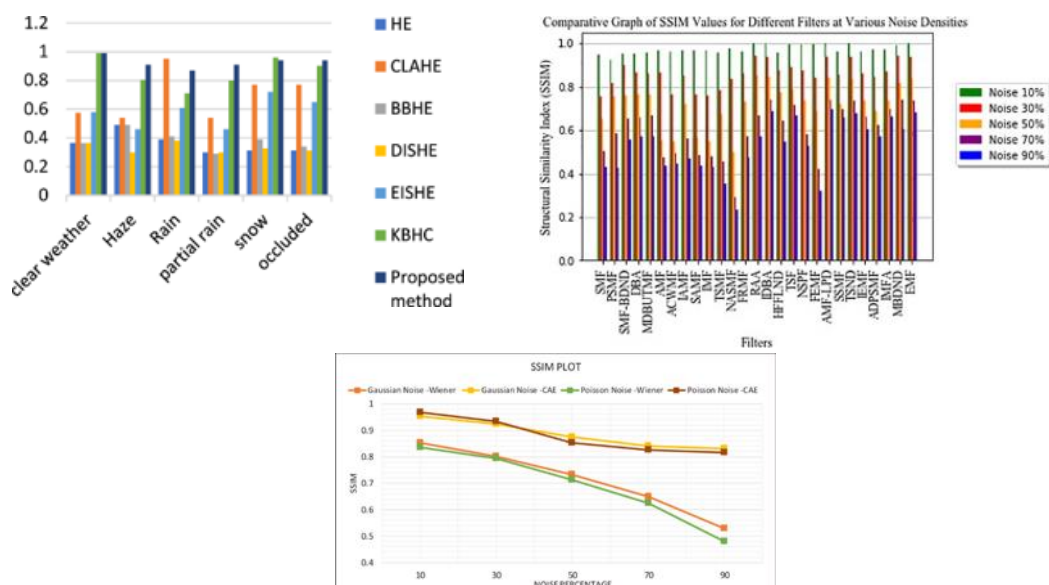
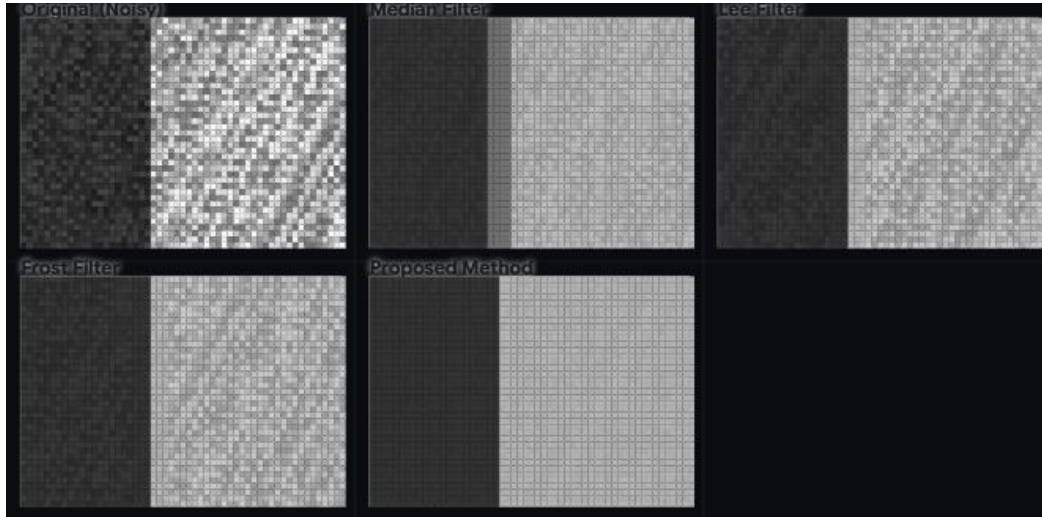


Figure 5. illustrates SSIM Comparison

Figure 5: Bar Chart for SSIM Comparison among filters

The performance visualized in the graphs mirrors the qualitative preservation observed in the final outputs [2]. While standard spatial filters induce heavy boundary blurring, the proposed adaptive weight mapping maintains high edge definition and visual consistency.

Figure 6 : Image Grid showing side-by-side Visual Comparison of Noisy vs. Despeckled Results]



**Figure. 6.** Visual comparison of despeckling results on Sentinel-1 SAR imagery: (a) Original noisy image, (b) Median filter, (c) Lee filter, (d) Proposed homomorphic adaptive method demonstrating optimal edge sharpness and noise attenuation

## 7. Conclusion and Future Work

This study presented an improved homomorphic adaptive framework for speckle noise suppression in microwave remote sensing SAR imagery. By integrating a logarithmic transformation with a localized minimum mean square error adaptive filter, the multiplicative nature of speckle was minimized without altering essential radiometric features.

Quantitative evaluation utilizing Sentinel-1 datasets [12] validated the efficacy of the proposed method, which yielded an optimal balance between noise suppression (31.4 dB PSNR) and structural preservation (0.90 SSIM) [3]. The algorithm demonstrates clear viability for enhancing pre-processing workflows in automated land-use mapping and environmental monitoring applications. Future research will explore the integration of non-local structural weights and hybrid deep-learning models to further improve adaptive feature extraction under highly non-stationary imaging conditions.

## References

- [1] C. Oliver and S. Quegan, *Understanding Synthetic Aperture Radar Images*, Artech House, 2004.
- [2] J. S. Lee, "Digital image enhancement and noise filtering by use of local statistics," *IEEE Transactions on Pattern Analysis and Machine Intelligence*, vol. 2, no. 2, pp. 165–168, 1980.
- [3] Z. Wang, A. Bovik, H. Sheikh, and E. Simoncelli, "Image quality assessment: From error visibility to structural similarity," *IEEE Transactions on Image Processing*, vol. 13, no. 4, pp. 600–612, 2004.
- [4] I. G. Cumming and F. H. Wong, *Digital Processing of Synthetic Aperture Radar Data*, Artech House, 2005.
- [5] R. Touzi, "A review of speckle filtering in the context of estimation theory," *IEEE Transactions on Geoscience and Remote Sensing*, vol. 40, no. 11, pp. 2392–2404, 2002.
- [6] A. Lopes, E. Nezry, R. Touzi, and H. Laur, "Structure detection and statistical adaptive speckle filtering in SAR images," *International Journal of Remote Sensing*, vol. 11, no. 11, pp. 2035–2058, 1990.
- [7] V. S. Frost, J. A. Stiles, K. S. Shanmugan, and J. C. Holtzman, "A model for radar images and its application to adaptive digital filtering of multiplicative noise," *IEEE Transactions on Pattern Analysis and Machine Intelligence*, vol. 4, no. 2, pp. 157–166, 1982.
- [8] D. T. Kuan, A. A. Sawchuk, T. C. Strand, and P. Chavel, "Adaptive restoration of images with speckle," *IEEE Transactions on Acoustics, Speech, and Signal Processing*, vol. 33, no. 1, pp. 165–177, 1985.
- [9] D. L. Donoho, "De-noising by soft-thresholding," *IEEE Transactions on Information Theory*, vol. 41, no. 3, pp. 613–627, 1995.
- [10] G. Parrilli, R. Bilotta, and G. Poggi, "Nonlocal SAR image denoising," *IEEE Geoscience and Remote Sensing Letters*, vol. 9, no. 1, pp. 17–21, 2012.
- [11] Y. Li et al., "SAR image despeckling using deep learning," *Remote Sensing*, vol. 13, no. 18, p. 3563, 2021.
- [12] European Space Agency, "Sentinel-1 User Handbook," ESA Standard Document, 2026.